Ferroelectric Compositions as Fast Switching Materials for Accelerator Applications

Norayr Martirosyan

CANDLE, 0040 Yerevan, Armenia
E-mail: n_martirosyan@asls.candle.am ; Tel.: +374 99 993349

Topics

- Fast Switching Ferroelectric Materials for Accelerator Applications
- Ferroelectric and Multiferoic materials
- Self-propagating High-temperature Synthesis (SHS)
- SHS of BaxSr1-XTiO3 and 0.77$BiFeO_3$-0.33$BaTiO_3$ Solid Solution
- Nanostructure production, based on BaxSr1-XTiO3 ferroelectrics.
- Dielectric characteristics of nanofilm Pt/BaxSr1-xTiO3/Pt structure under electron beam irradiation

The Type Scheme of RF Phase Rotator/Shifter

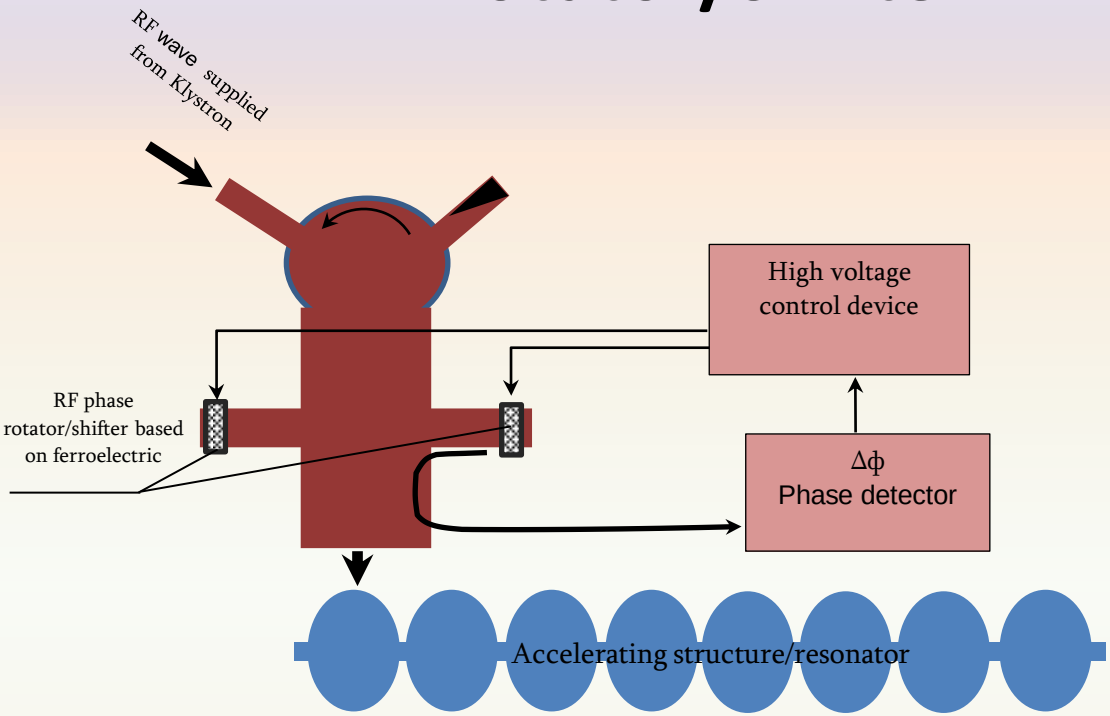

- ✓ The ferroelectric-based high power RF shifter is 1-2 times quicker than the usual ferrite or mechanical regulators.

Prototype BST(M) Ferroelectric Ring Sample and Conceptual Layout of the Switch

The ring diameter is 110 mm, thickness is 2.8 mm. The 2 um thick gold biasing contact deposited on the ring edge.

The operating mode of the cavities is TE_{031}

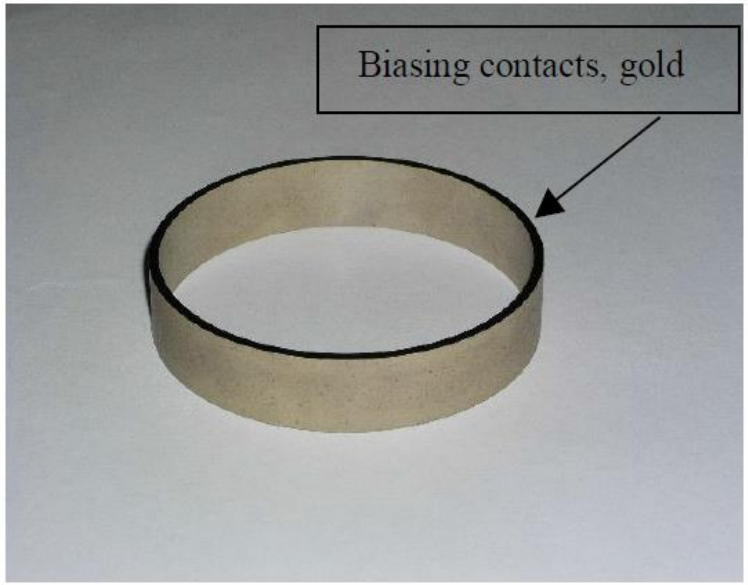

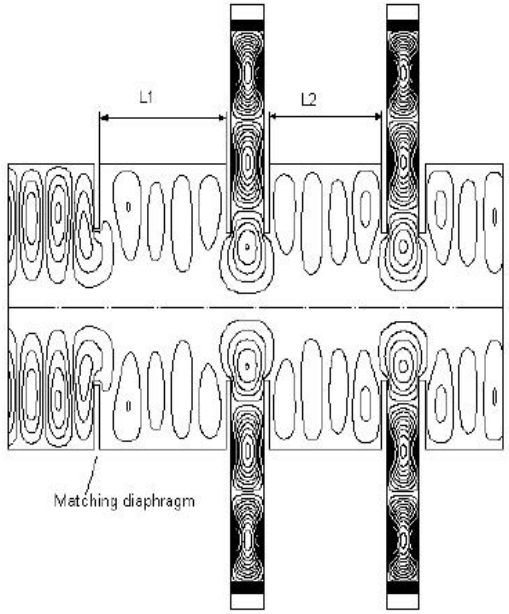

A. Kanareykin, E. Nenasheva, V. Yakovlev & et al.

Basic Designs of Tunable Dielectric Loaded Accelerating Structures

(a): Cylindrical geometry, with ferroelectric outer layer and ceramic inner layer. The thickness of the ferroelectric layer is 1/10 of the ceramic thickness. (b): Tunable planar structure geometry.

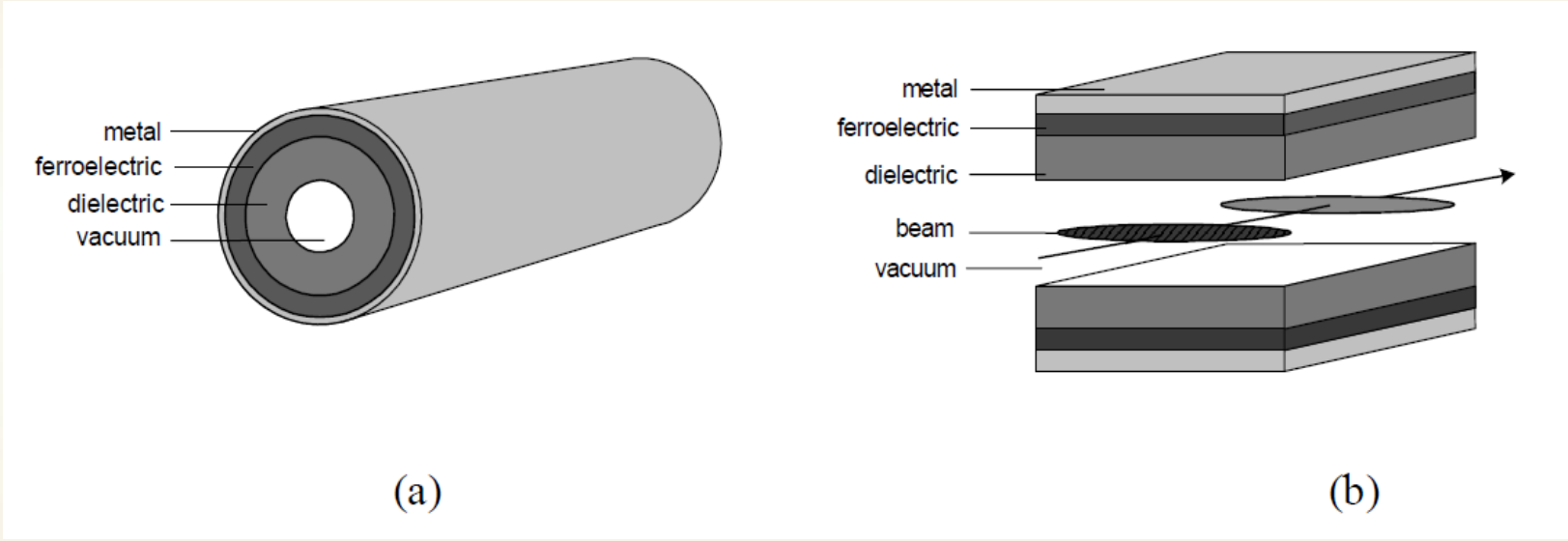

A. Kanareykin, E.Nenasheva, S.Karmanenko, V.Yakovlev

Properties of $Ba_xSr_{1-x}TiO_3$ (x=1; 0.5; 0.4)

Dielectric constant at 10 GHz	400…500
Dielectric loss at 3-11 GHz	0.0021…0.0068
High electric breakdown strengths	100…200 kV/cm
Bias electric field	20…50 kV/cm
Tunability factor at 50 kV/cm	1.15 – 1.20
Leakage current density at a field intensity of 2×10^5 V cm^{-1}	$10^{-11} \dots 10^{-10}$ A cm^{-2}

Ferroelectric and multiferoic

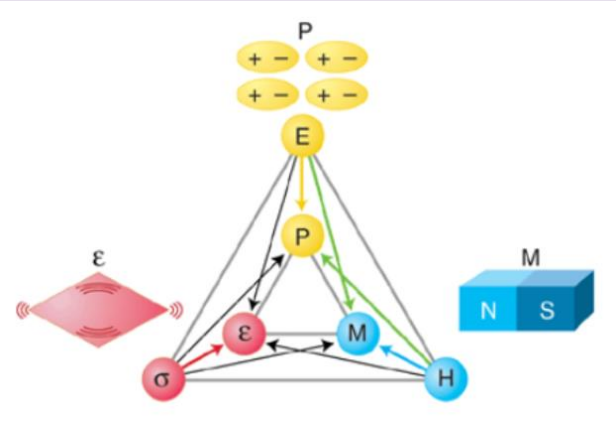

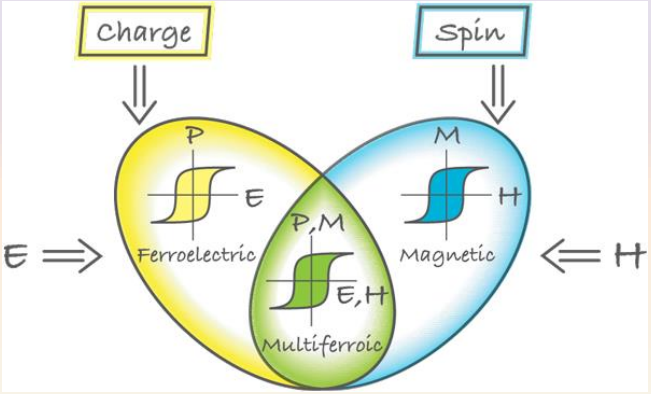

- Ferroic: P, M or ε are spontaneously formed to produce ferroelectricity, ferromagnetism or ferroelasticity;
- Multiferroic: Multiferroics are defined as materials with at least two of the forms of primary ferroic order in the same phase. Multiferroics combine the properties of ferroelectrics and magnets.

In the ideal case, the magnetization of a ferromagnet in a magnetic field displays the usual hysteresis (blue), and ferroelectrics have a similar response to an electric field (yellow). $0.77BiFeO_3$-$0.33BaTiO_3$ are simultaneously ferromagnetic and ferroelectric, there is a magnetic response to an electric field.

Since multiferroics combine magnetic and electric properties in the same phase and can present a coupling between the magnetic and electric properties, they provide a new perspective for devices design and can be used to construct new RF phase rotator/shifter (phase and amplitude modulator) based on the simultaneously change of dielectric and magnetic penetration in ferroelectric under the impact of external field.

SHS Powder Production Technology

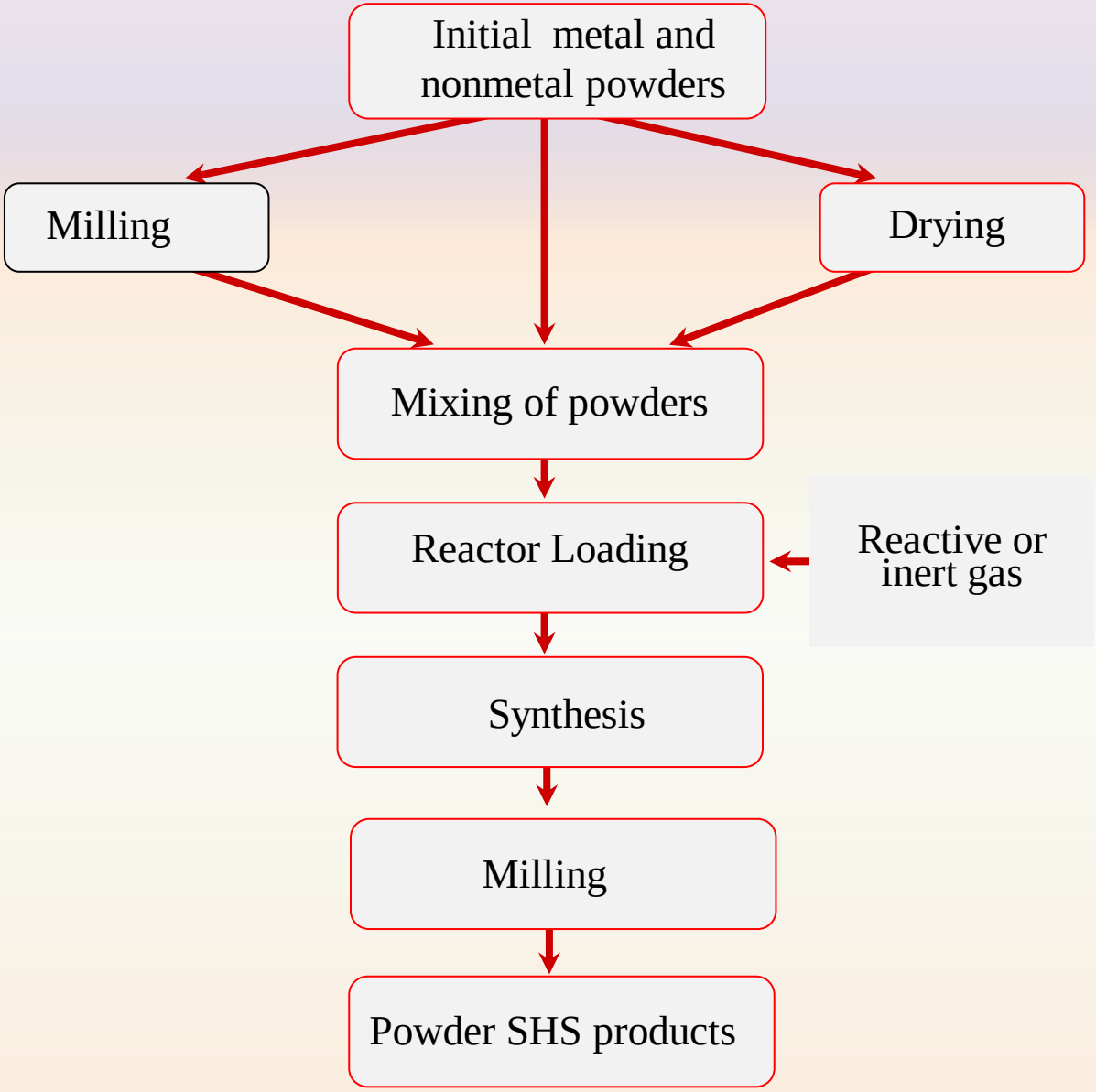

The technological scheme of powder production includes the following operations:

- preparation of a green mixture;
- milling, drying of components;
- mixing;
- filling of a reactor with a green mixture and gases;
- synthesis after a short–time thermal initiation;
- subsequent processing of synthesized products;
- milling, drying.

SHS Technological Types are Characterized by the Following Features:

- low energy consumption (in most cases it is only necessary for initiating an SHS process);
- simple technological equipment, it has high productive capacity and safety;
- decreased number of technological stages in comparison with conventional technologies;
- feasibility of production lines adaptable to the production of different materials and items and amenable to mechanization and automation;

Experimental SHS Reactor

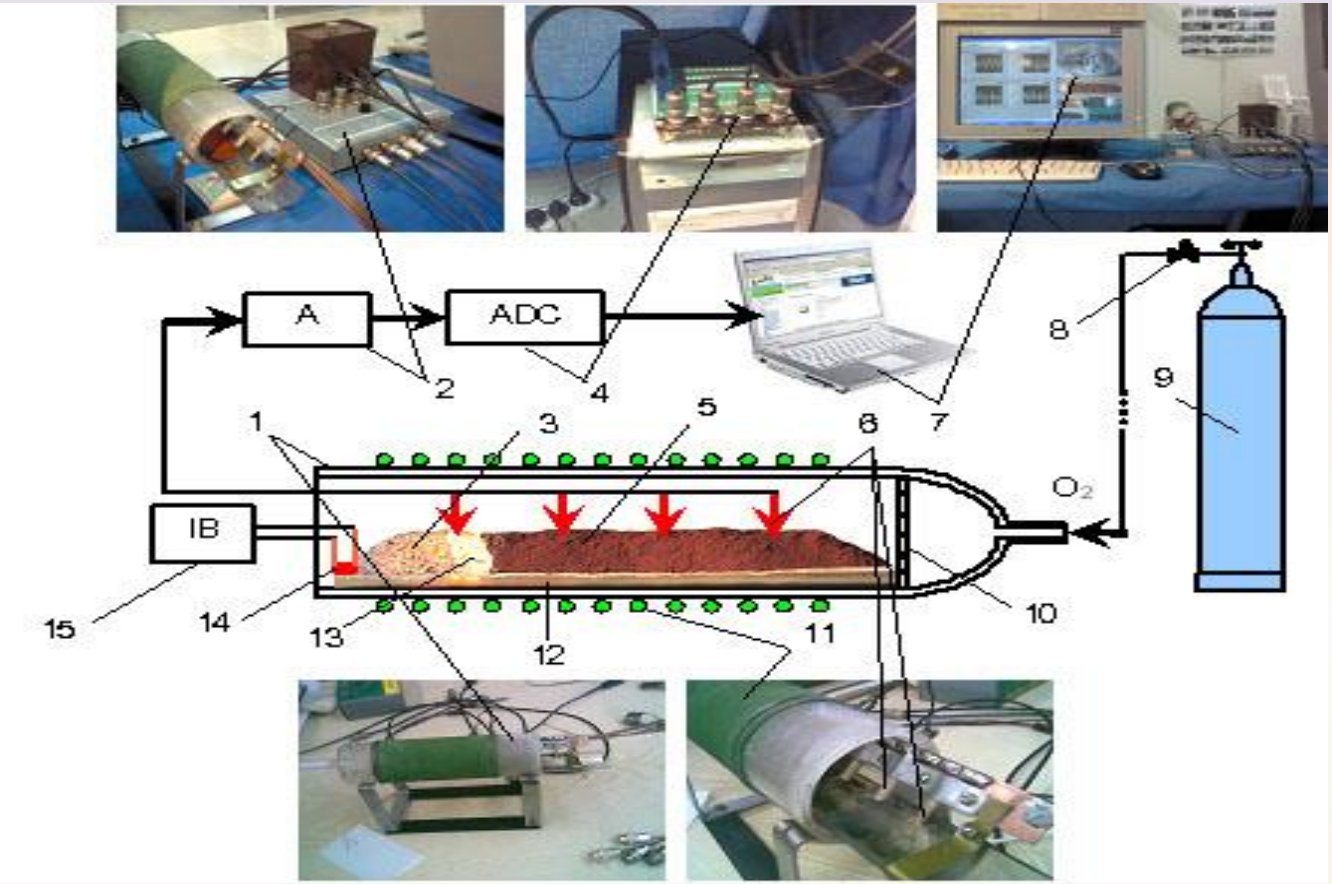

1. Quartz tube; 2. low noise amplifier; 3. end product; 4. analog-digital convertor; 5. green mixture; 6. thermocouples; 7. PC; 8. oxygen flow controller; 9. oxygen; 10. quartz mesh; 11. heater; 12. thermoresistant boat; 13. combustion front; 14. wolfram ignitor; 15. ignition block.

Temperature Distribution Along Combustion Front Propagation

I-green mixture; II-warming-up zone; III-metal oxidation zone; IV-active oxidation of metal and formation of the intermediated; V-zone of secondary chemical interactions between intermediates and formation of final product; VI-cooling-down zone.

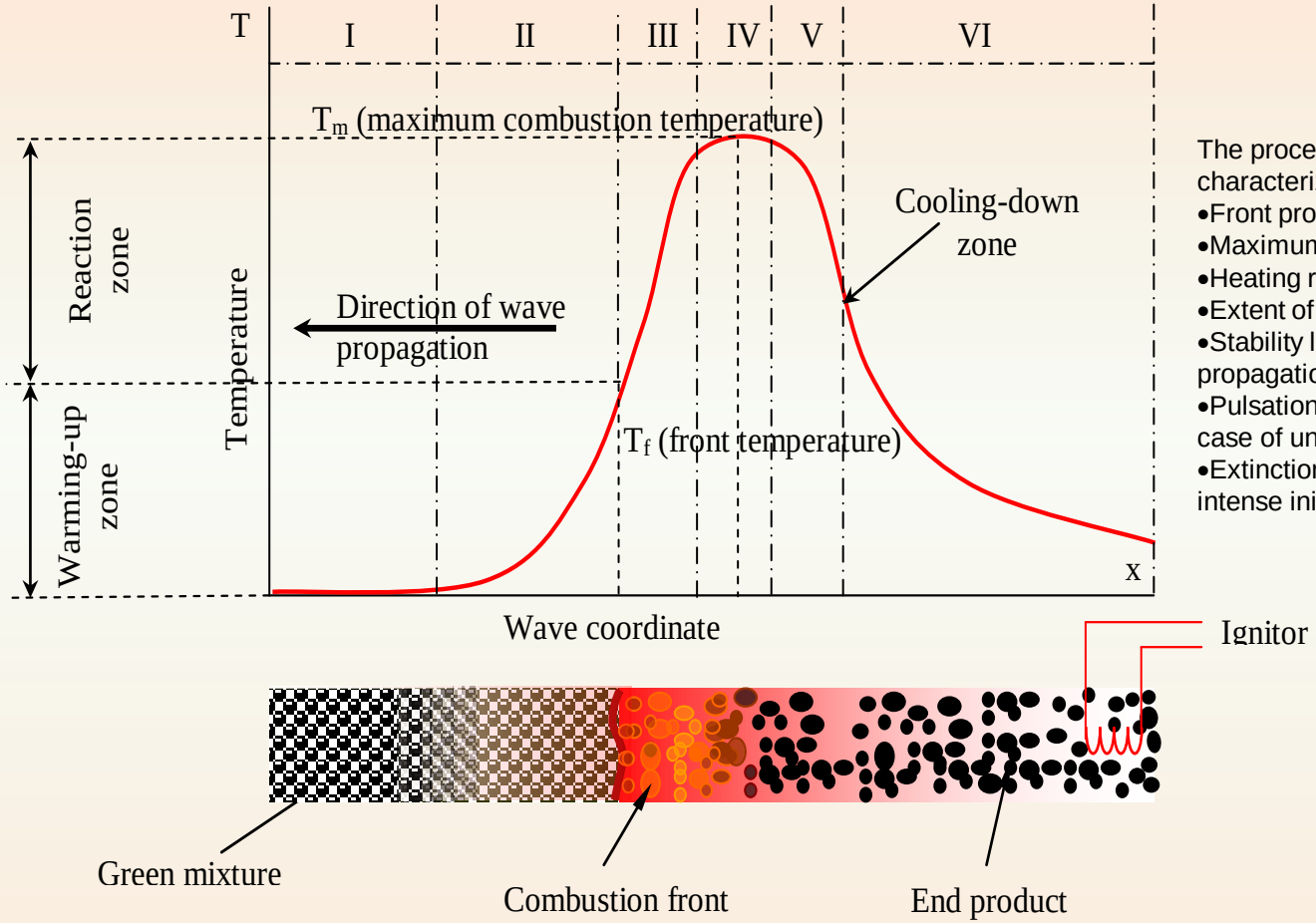

The process of wave propagation is characterized by:

- Front propagation (burning) velocity.
- Maximum combustion temperature.
- Heating rate in the combustion front.
- Extent of phase/structure transformation.
- Stability limit (steady or unsteady wave propagation) .
- Pulsation frequency, hot spot velocity, etc. (in case of unsteady combustion).
- Extinction limit (no combustion even upon intense initiation).

The Synthesis were Done According to the Following Chemical Schemes

- $x BaO_2 + (1-k) TiO_2 + k Ti + (1-x) SrCO_3 + O2 \rightarrow Ba_xSr_{1-x}TiO_3$

- $[1-y][(1-x)(1/2Bi_2O_3+(1-K)/2Fe_2O_3+KFe)+x(BaO_2+(1-k)TiO_2+kTi)]+yMnO_2+O_2=[1-y][(1-x)BiFeO_3–xBaTiO_3]-yMn$

Combustion temperature (T_c) and velocity (U_c) *vs.* amount of combustible (Ti) in the initial mixture for $Ba_{0.25}Sr_{0.75}TiO_3$

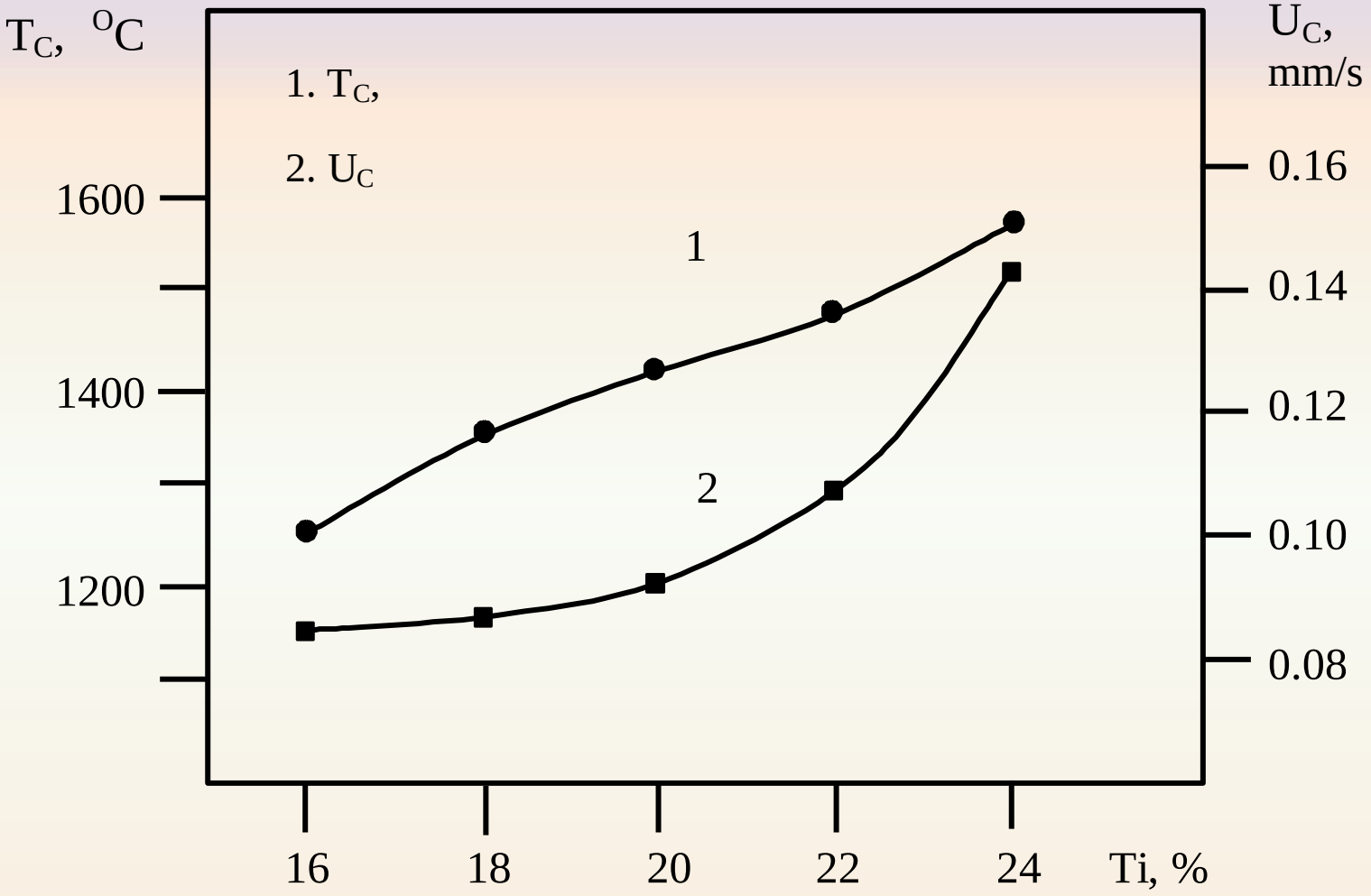

Combustion temperature (Tc) and velocity (Uc) vs. amount of the combustible in the initial mixture for

$0.3BaTiO_3 – 0.7BiFe_{0.97}Mn_{0.03}O_3$

a) Ti is 2%; b) Fe is 2%.

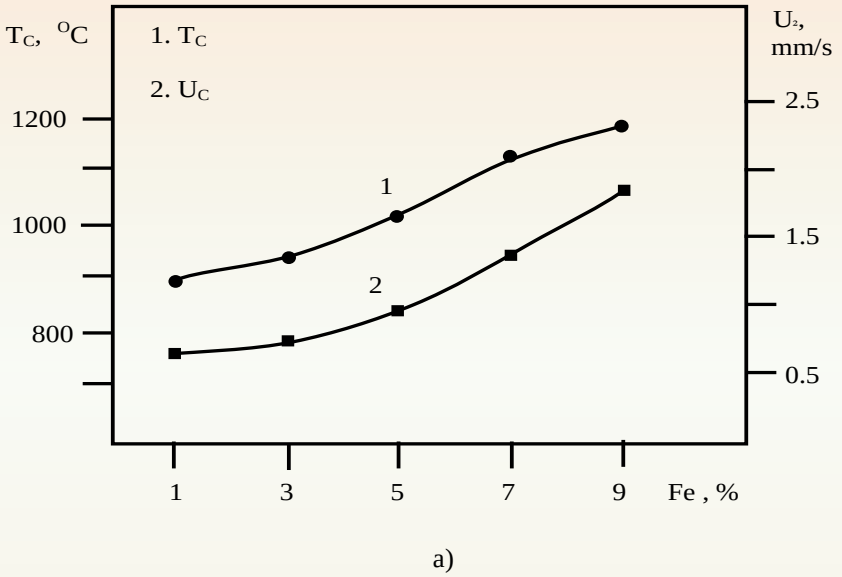

a)

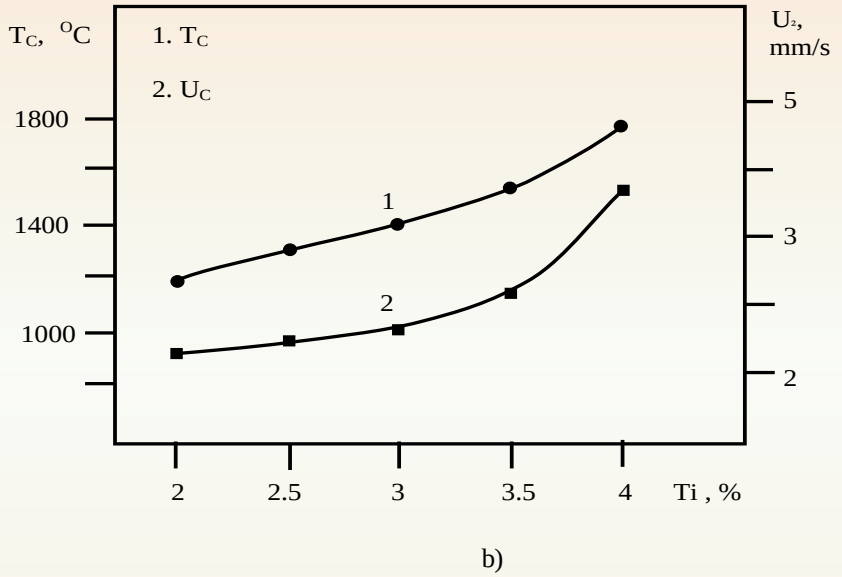

b)

XRD patterns of $Ba_{0.25}Sr_{0.75}TiO_3$ powder

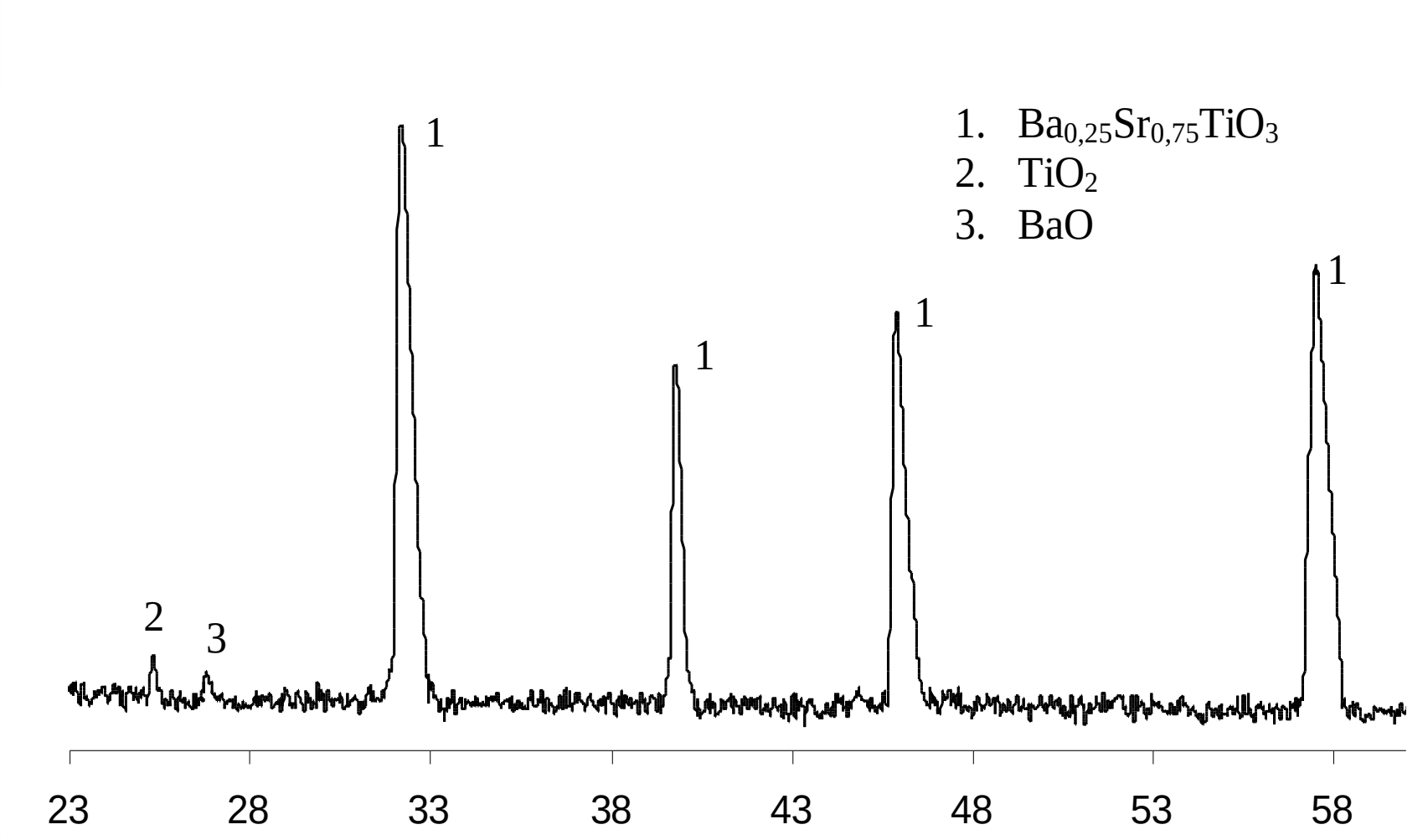

Relative intensity vs. amount of the combustible in the initial mixture for $0.3BaTiO_3 – 0.7BiFe_{0.97}Mn_{0.03}O_3$ composition

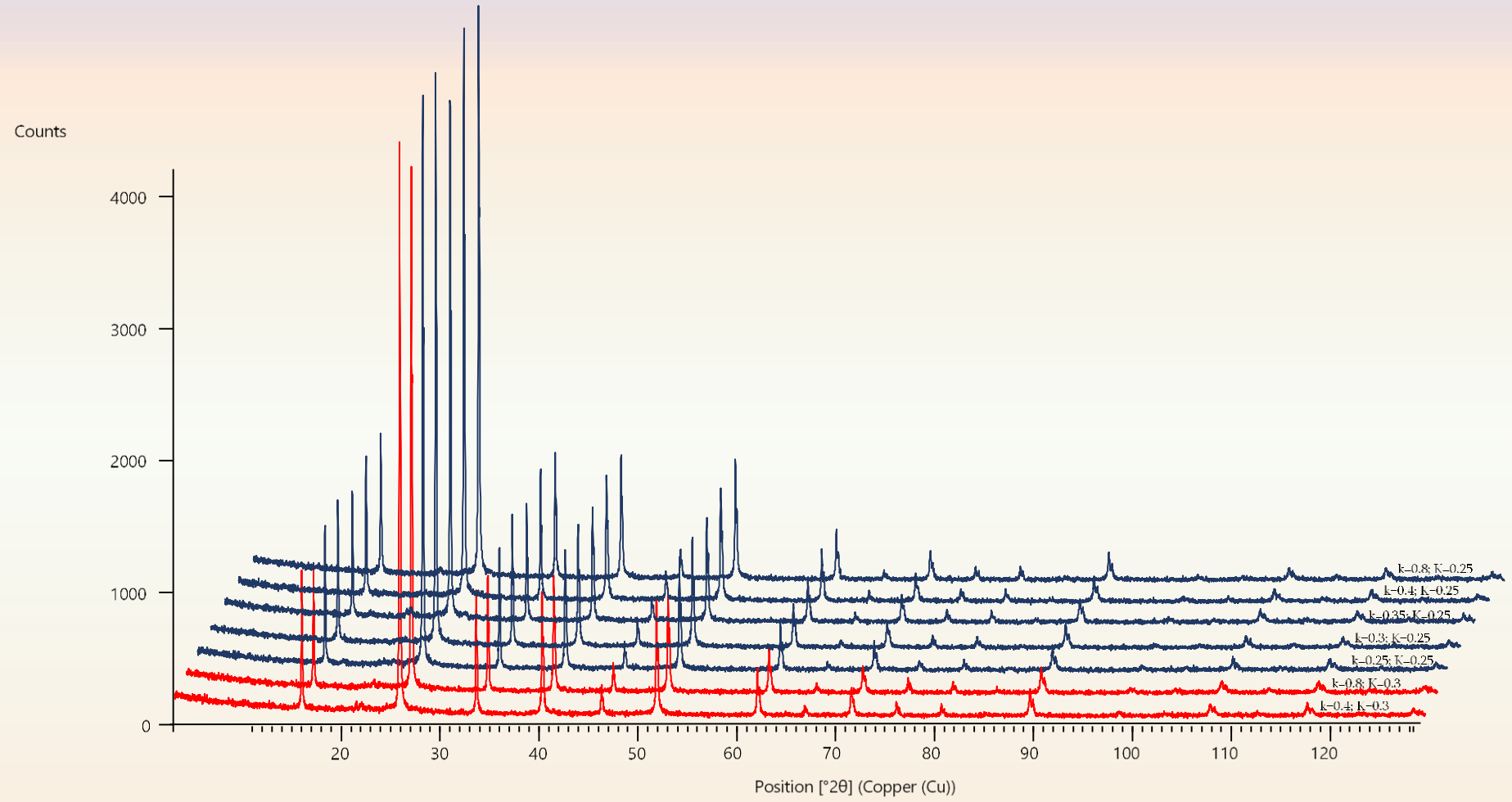

SEM images of $0.3BaTiO_3$-$0.7BiFe_{0.97}Mn_{0.03}O_3$ compositions after SHS

a) K=0.2, k=0.2; b) K=0.3, k=0.6.

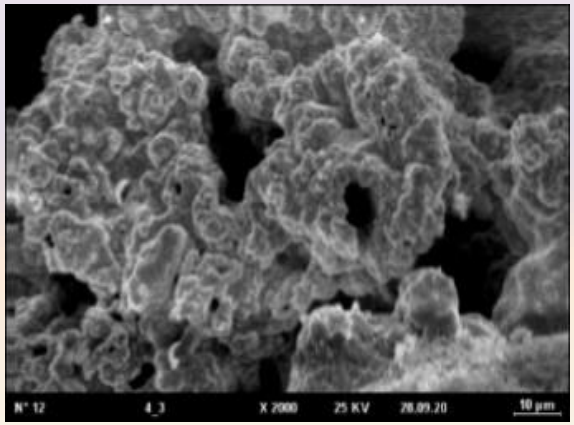

a)

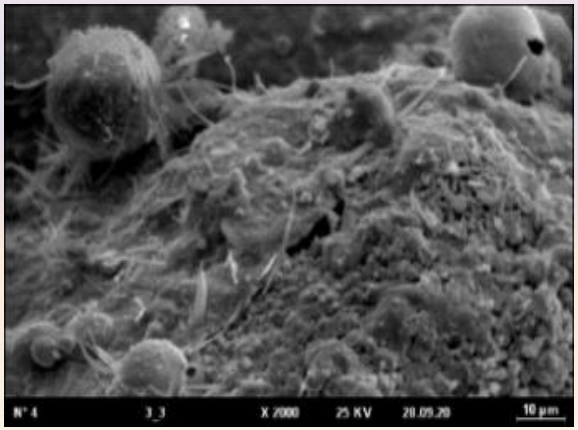

b)

SEM images after grinding by PULVERISETTE 6 planetary ball mill

The milling duration is a)- 6 hours, b)- 7 hours.

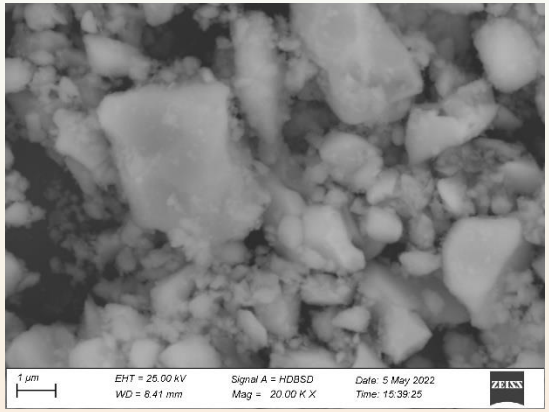

a)

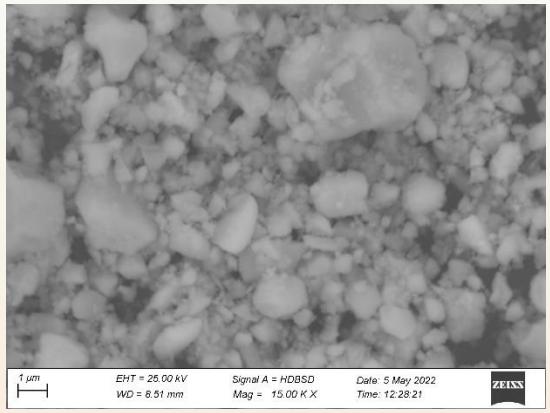

b)

The shape and the size of compacts are disks of 6…12 mm in diameter and 5...7 mm thick

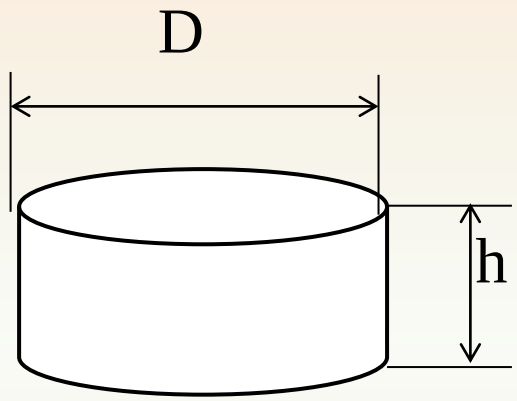

The linear shrinkage factor and density of 0.3BaTiO3-0.7BiFe0.97Mn0.03O3 ceramic samples vs. sintering temperature.

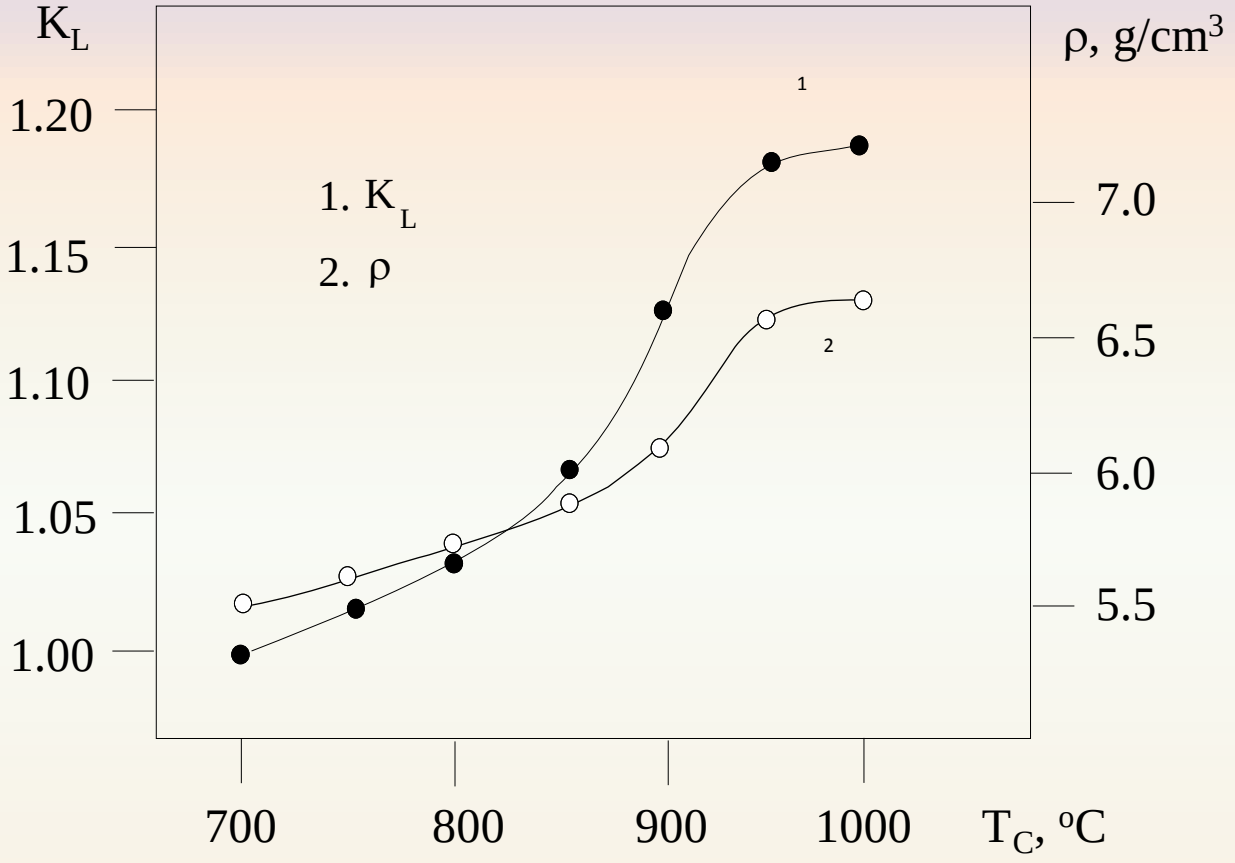

Linear shrinkage factor of $Ba_{0.25}Sr_{0.75}TiO_3$ ceramic samples vs. sintering temperature

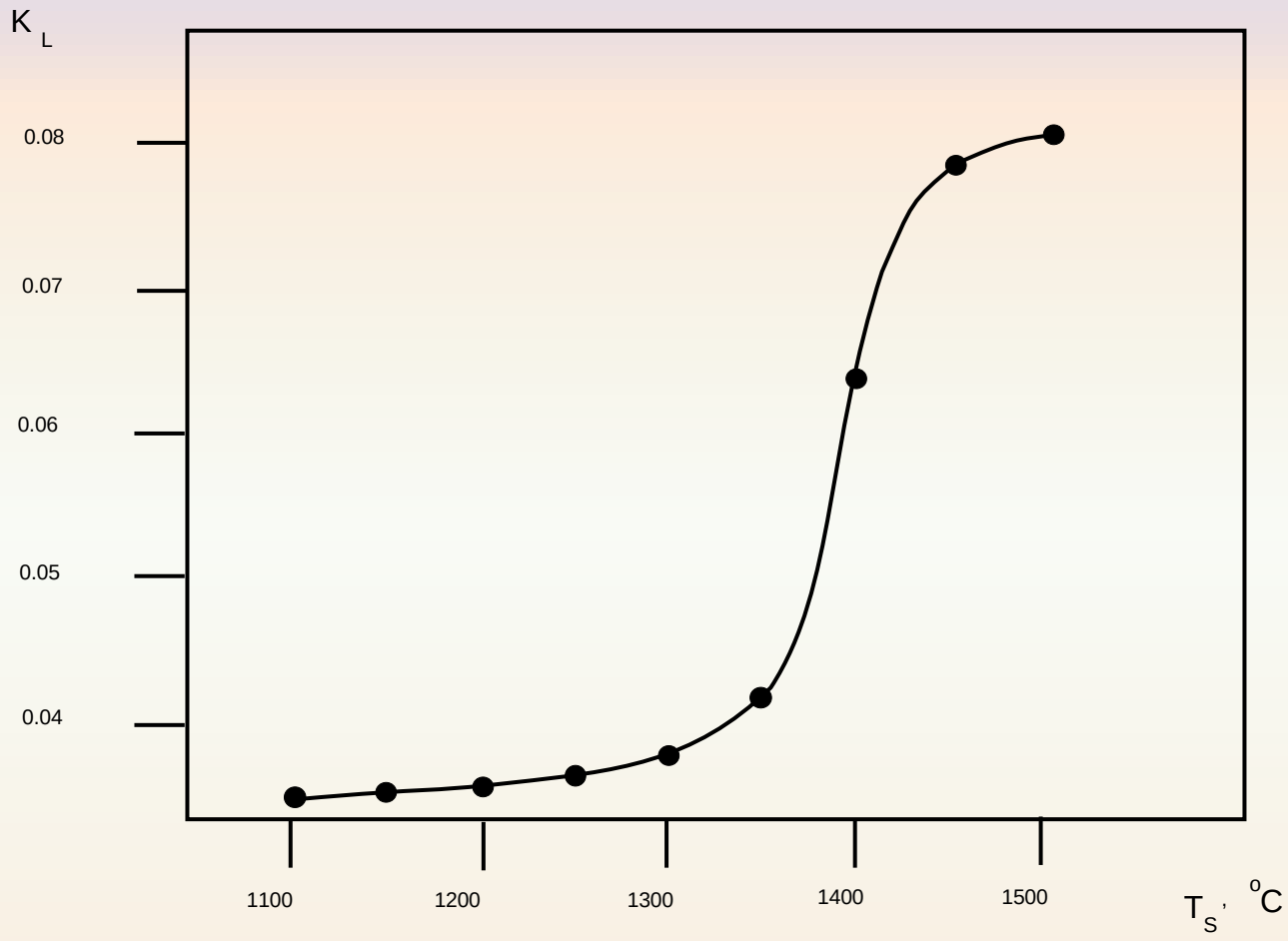

SEM image of $0.7BiFe_{0.97}Mn_{0.03}O_3–0.3BaTiO_3$ ceramic sample pressed under 5000 kg/cm^2 pressure and sintered at 950 °C

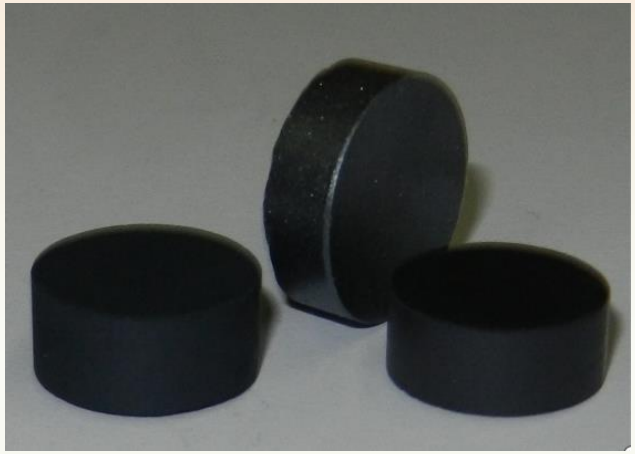

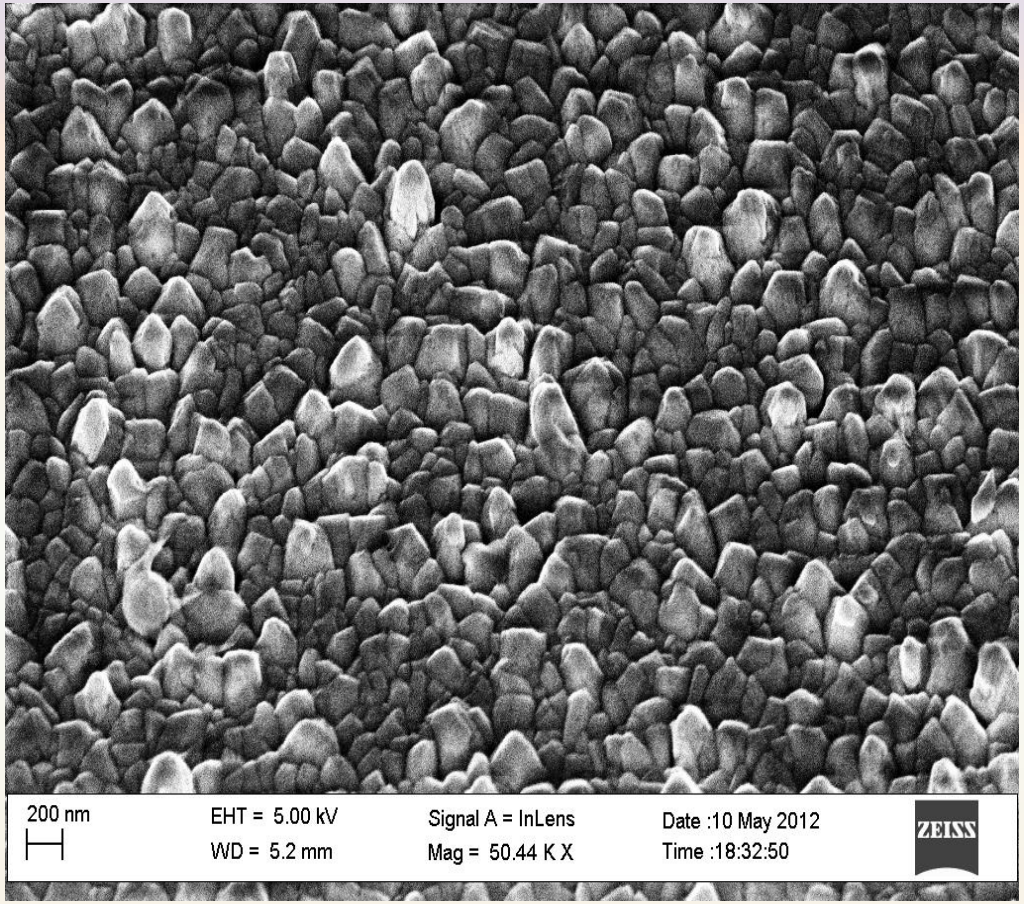

SEM image of $Ba_{0.25}Sr_{0.75}TiO_3$

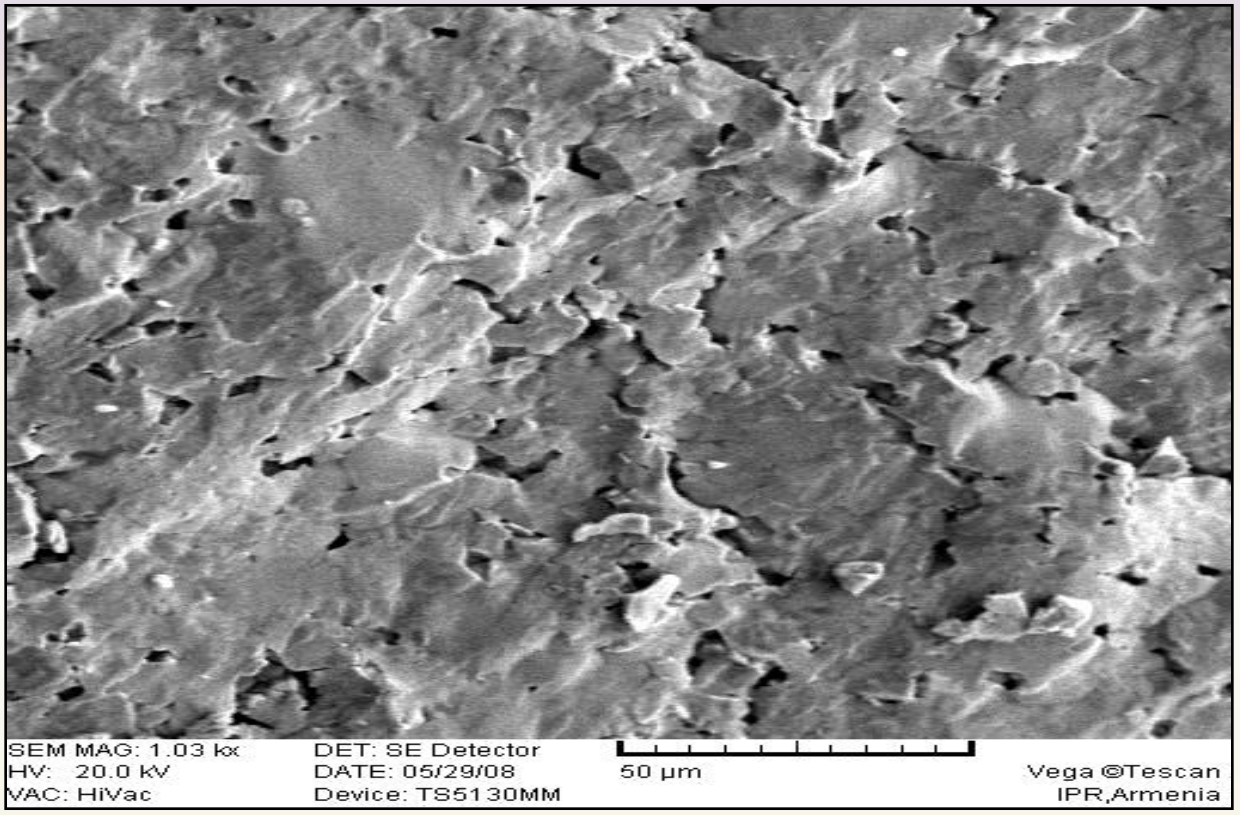

The tunability factors (ε(0)/ε(E) and μ (0)/ μ(E)) of 0.3BaTiO3-0.7BiFe0.97Mn0.03O3 ceramic sample vs. biasing field (at 30 MHz)

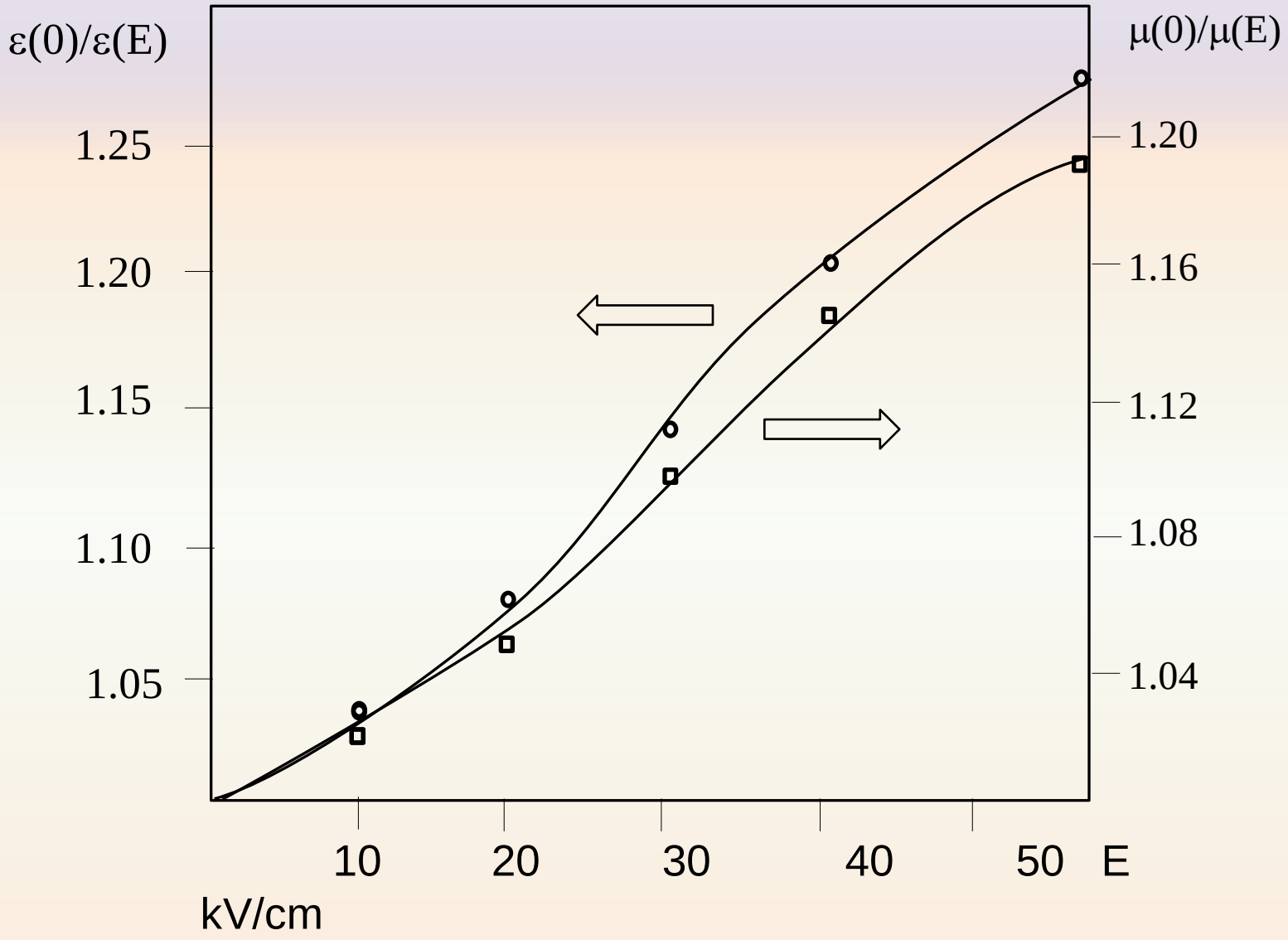

PLD of $Ba_{0.25}Sr_{0.75}TiO_3$ on a silicon substrate (p-Si, ρ = 1000 Ωcm)

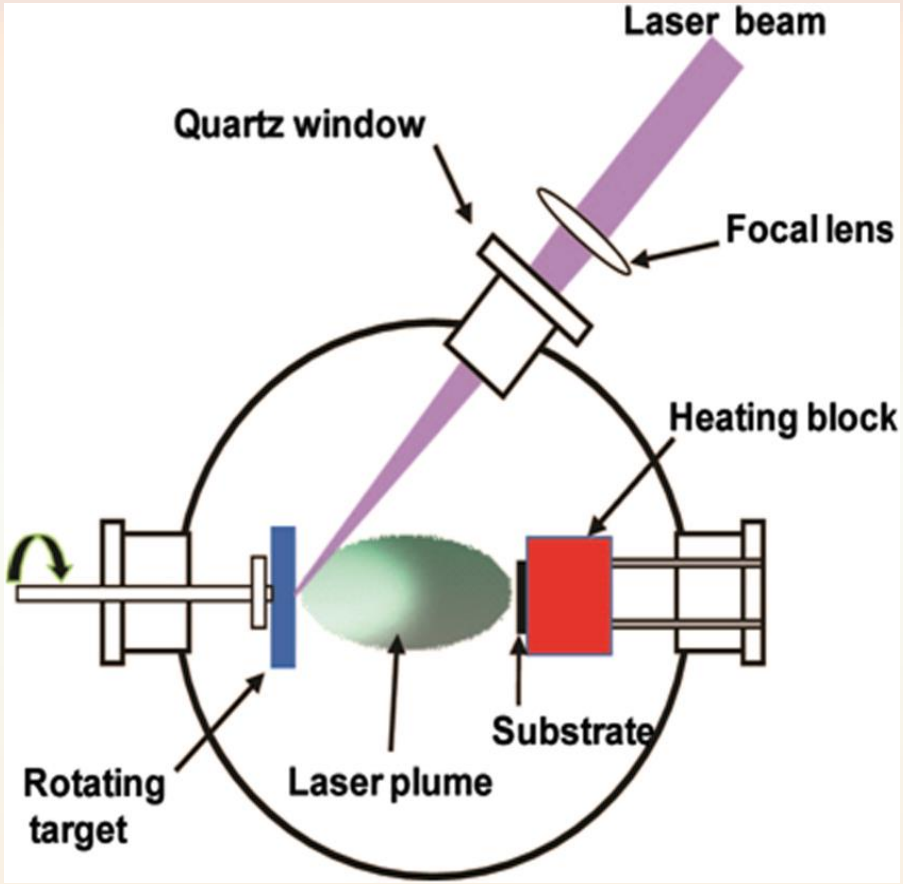

- Oxygen flow 30 mL/min, pressure $2x10^{-3}$ mbar;
- KrF-excimer laser (Lambda LPX305) with a pulse width of 20ns ;
- Pulse energy of approximately 1J per pulse;
- Energy density of 2.5Jcm^{-2} ;
- Repetition rate of 10Hz;
- Deposition time of 100s.

Cross-sectional SEM image showing the Si-SiO2-Ti-Pt-BST layer stack

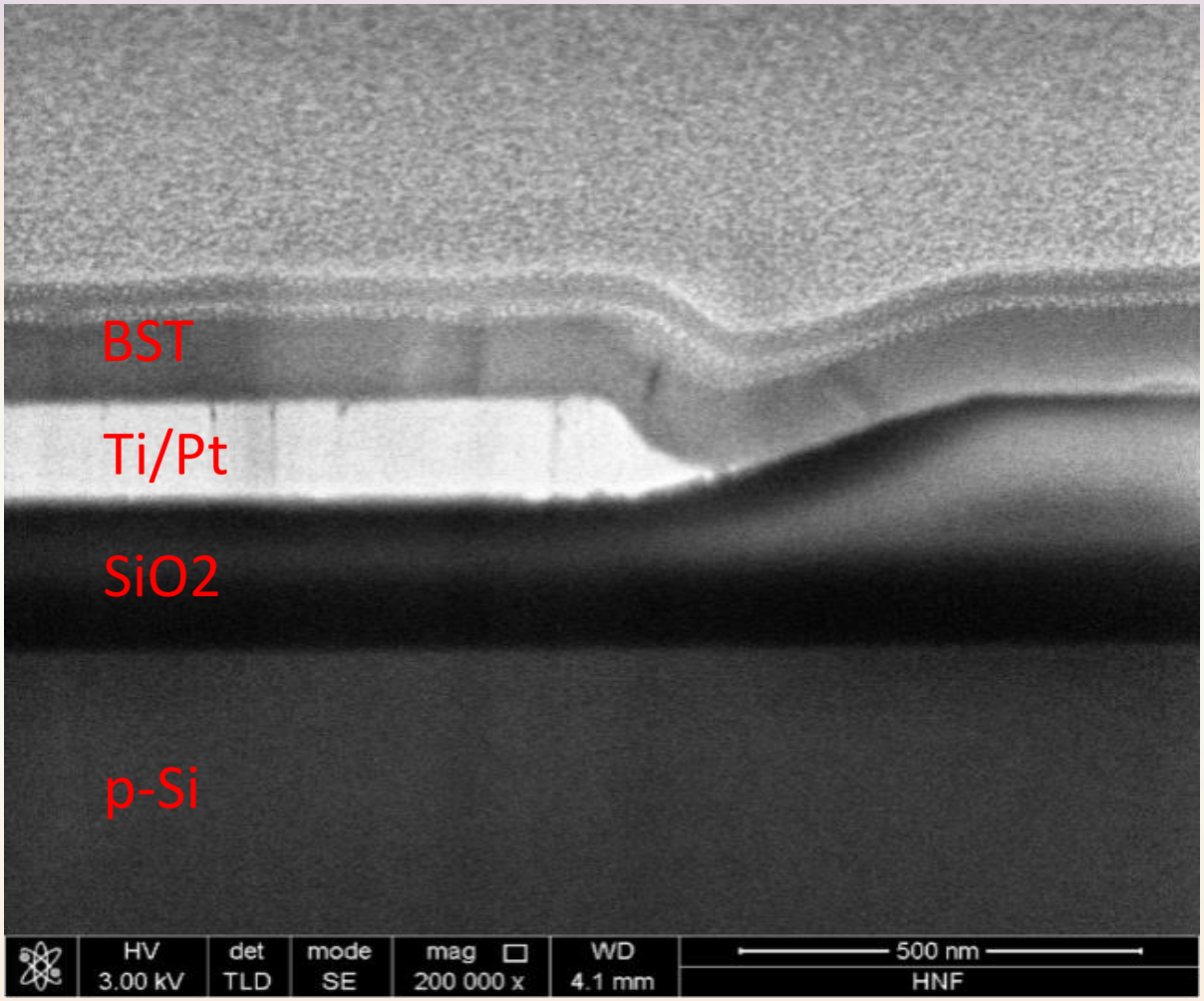

XRD patterns of $Ba_{0.25}Sr_{0.75}TiO_3$ nano-layer

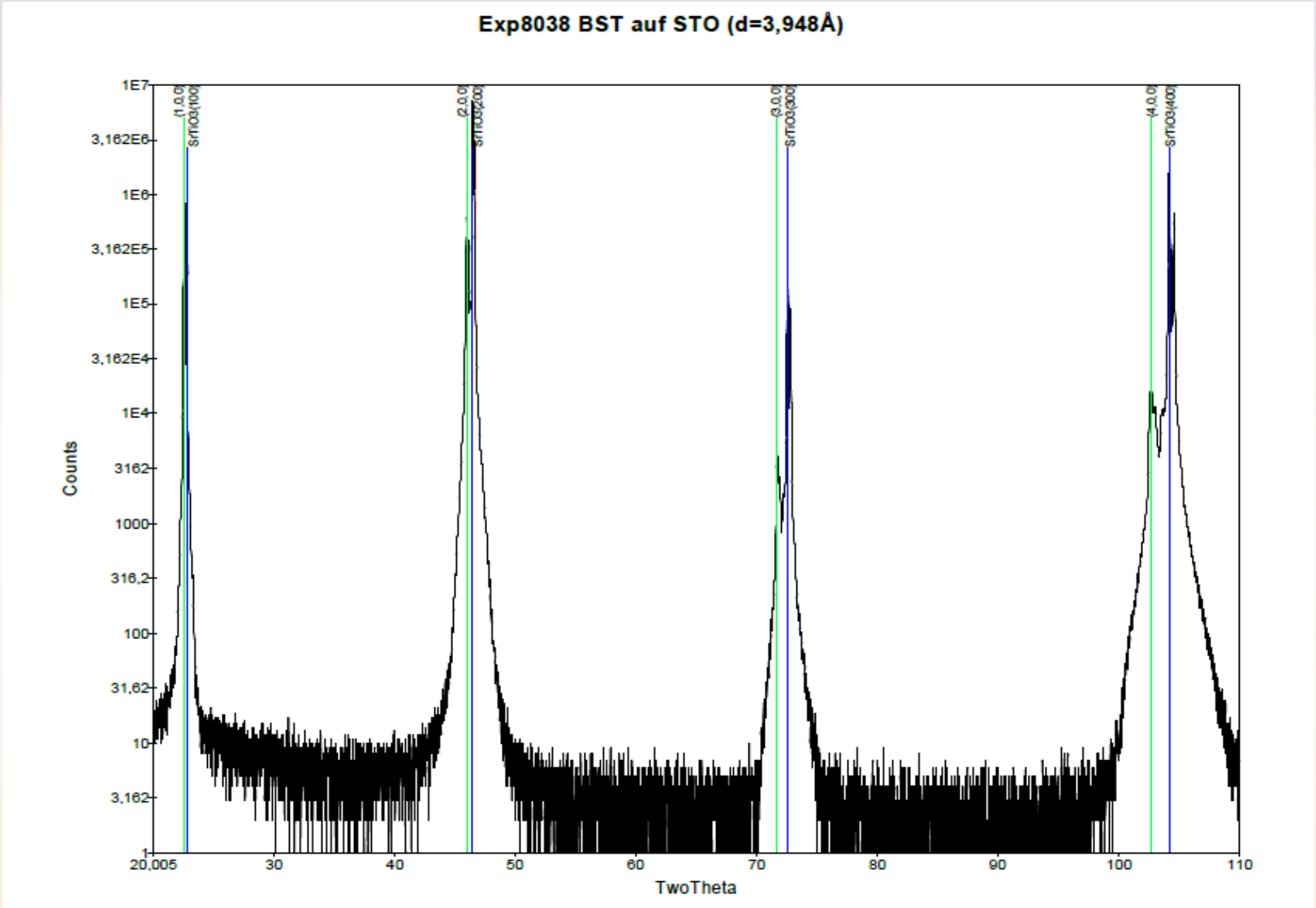

Photograph of a fabricated nano-layer structure chip - (b) and sizes of IDE geometry - (a)

a)

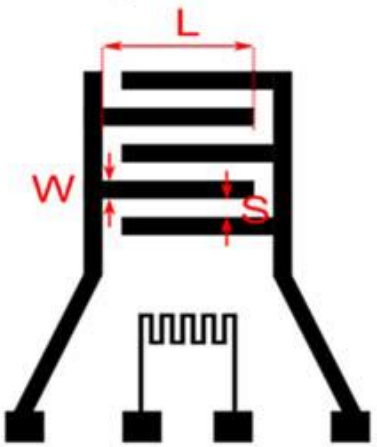

Finger number	50
Finger width W	600 μm
Finger spacing S	324 μm
Finger length L	2900 μm
Surface area A	0.087 μm
Substrate, SiO_2	500 μm
Ti / Pt	(20 / 200) nm
BST	485 nm

b)

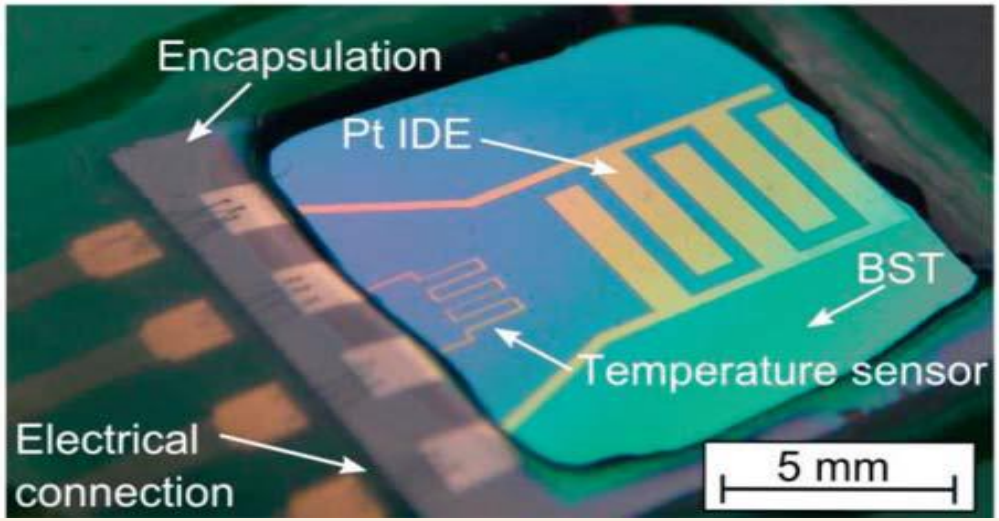

AREAL machine parameters for Electron Beam Irradiation

RF System			
RF High Voltage	[kV]	132	
RF High Voltage (Peak Power)	[dBm]	-4.02	Power meter on Gun
RF Phase	[deg]	-38	
Pulse Repetition Rate	[Hz]	12	
Magnets			
Solenoid Current	[A / V]	9.6/45	
Dipole Current	[A / V]	4.2/9	
Corrector Magnet (X | Y)	[A / V]	2.91/8	
Beam Parameters			
Beam Charge (FC-IN / FC-OUT)	[pC]	255/53	30 (absorbed by sample)
Beam Energy spectrometer	[MeV]	3.7	
Laser System			
Laser pulse duration	[ps]	0.5	
Time		1 hour	
Beam Profile @ YAG 1 (straight screen)		***Beam profile @ spectrometer E=3.7 MeV***	

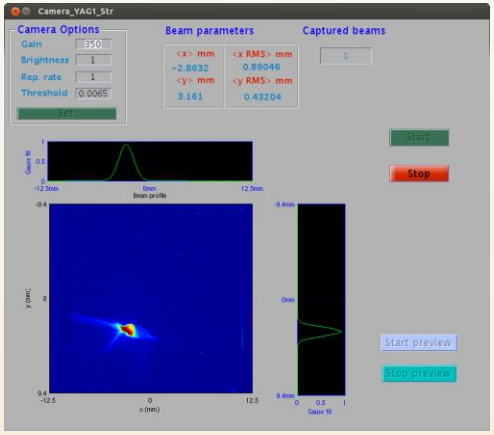

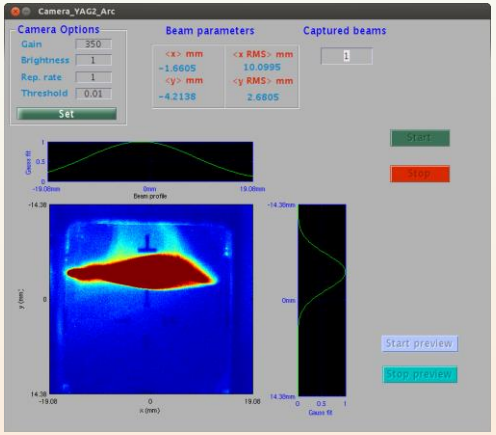

The C–f dependences of the examined structure

Before-blue line; after the first irradiation-red;
after the second irradiation-green; after the third irradiation-purple.

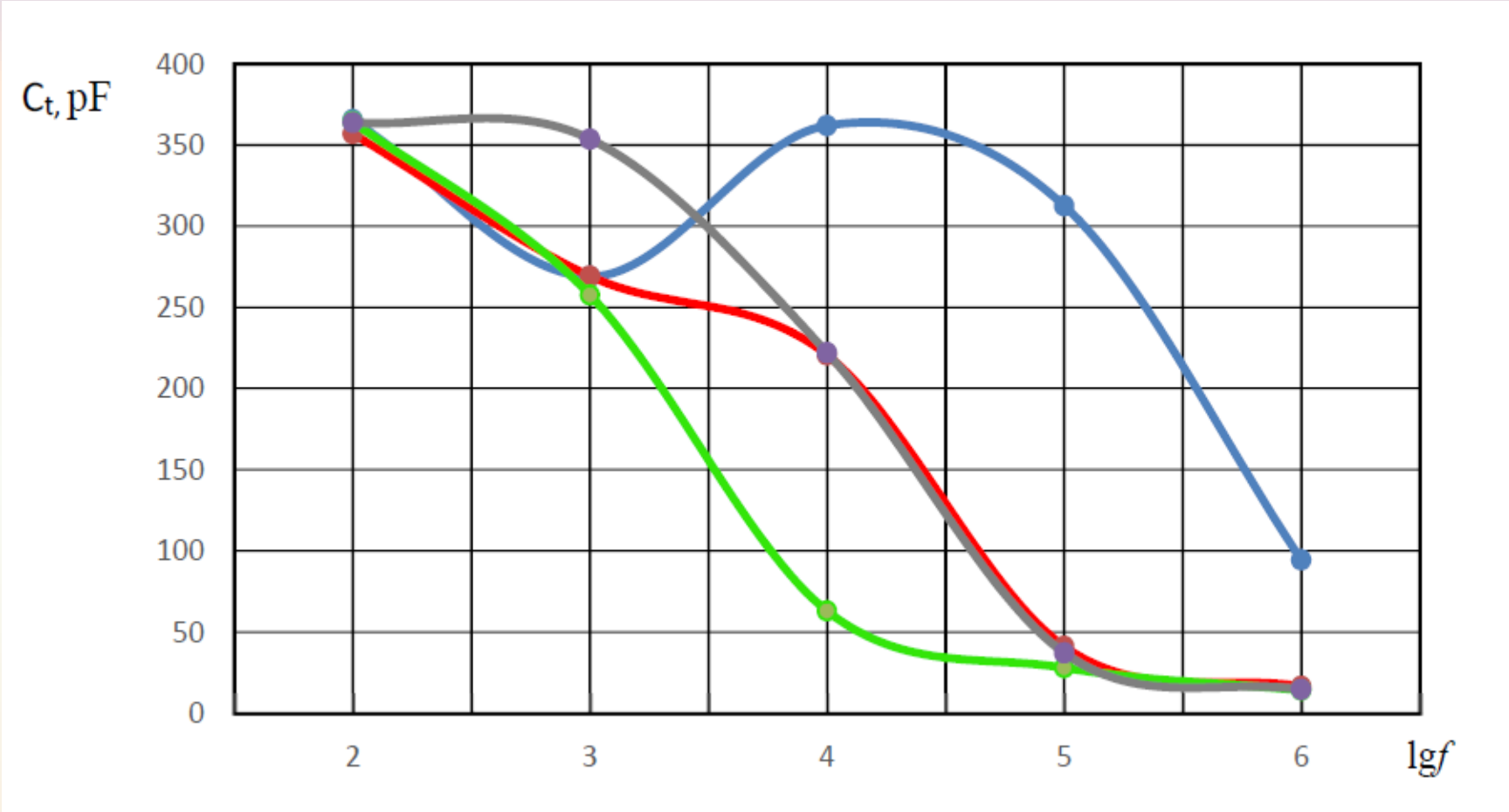

The calculation of ε_f *of the examined structures*

Equivalent circuits of the examined structures

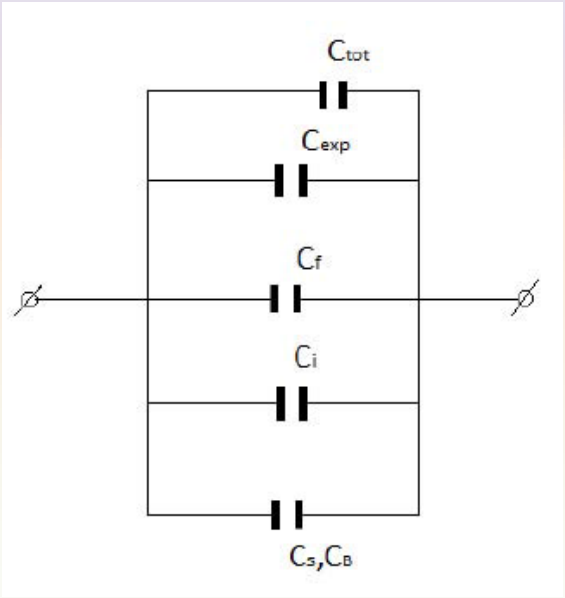

The total (measured) capacitance of the structure:

$$C_{tot} = (n-1)l \cdot C_1$$

n is the amount of fingers, l is the length of the fingers.

$$C_1 = \frac{\varepsilon_o \varepsilon_f}{2} \cdot \frac{K[(1-k^2)^{1/2}]}{K(k)} = \frac{\varepsilon_o \varepsilon_f K(k^1)}{2 \cdot K(k)},$$

$K(k)$is the complete elliptic integral of the fins t kind with modules of k.

$$k = \cos\left(\frac{\pi}{2} \cdot \frac{w}{w+S}\right).$$

The capacitance of the equivalent circuit of structure:

$$C_{tot} = C_s + C_\beta + C_f + C_{exp} + C_i,$$

where C_s is the capacitance of the substrate(pS_i), C_β is the parasitic capacitance between P_t electrodes (fingers), C_f is the capacitance of ferroelectric film, C_{exp} is the capacitance of the measurement set-up, C_i is the insulator lager (SiO_2) capacitance. The numerical calculations of C_i, C_β is shows, that its value about two order less than that the C_f and ignoring also the C_s , C_β and C_{exp}, we used the approximation of:

$$\varepsilon_f \cong \frac{2C_{tot}}{\varepsilon_o \cdot l \cdot (n-1)} \cdot \frac{K(k)}{K(k^1)}$$

The ε_f –f dependences of the examined structures

Before-blue line; after the first irradiation-red; after the second irradiation-green; after the third irradiation-purple.

The tanδ*–f dependences of the examined structures*

Before-blue line; after the first irradiation-red;
after the second irradiation-green; after the third irradiation-purple.

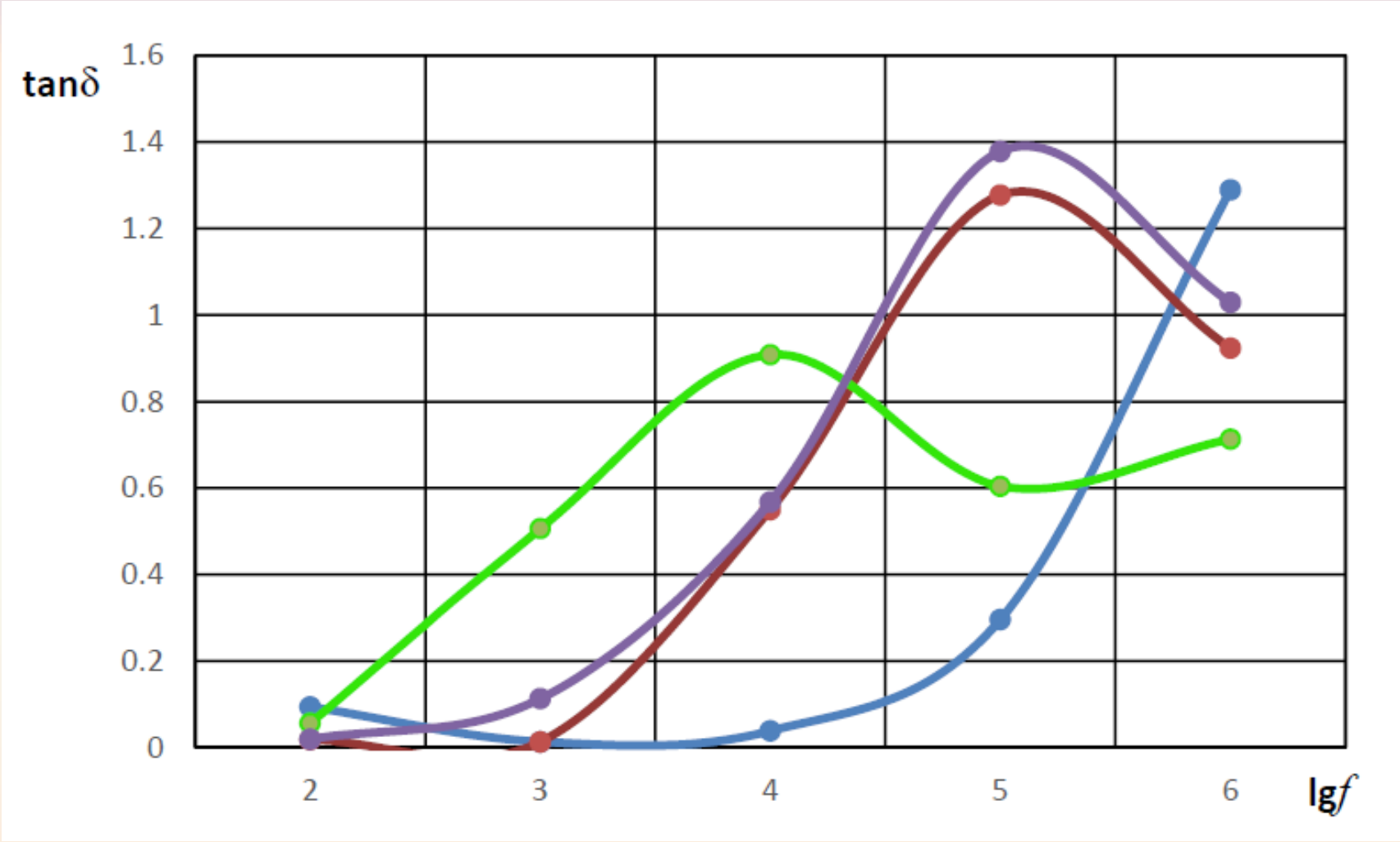

SUMMARY AND CONCLUSION

- It is established that the threshold value for k is 0.5 (if K=0) and for K is 0.25 (if k=0), only at greater values of k and K, the process can proceed under the self-sustaining mode.
- The phase structure investigation shows no other phases when the amount of combustible was about 10% (where Fe-8%, Ti-2%).
- As a result of calculations and series of experiments, it is determined that optimal grinding regimes and conditions are as follows: the volume relationship of the charge (material to be milled) and milling bodies/balls should be 1/4…1/3; acetone has to be used as a milling medium to form a freely flowing cream. Efficient milling is obtained when the volume of acetone is between 100 and 200% of the volume of the charge. The quantity of the grinding body/ball has been taken 70% of pots volume. The milling body/ball were of 4...8 mm in size (the largest diameter being of the order of a tenth of the diameter of the pot). The rate of the rotation (ωd) of the base disk is 400…600 rev/min. The milling duration is 7 hours.
- BF–BT based pellets are sintered between 700 °C and 1000 °C in an electric furnace and air atmosphere for 2 hours under controlled heating/cooling rates of 2.5 °C/min.
- The dependence for linear shrinkage factor and gas-penetrability of the samples vs. sintering temperature indicates that intensive sintering begins with 880 °C, and the maximum density of the samples is practically obtained at 950 °C.
- The tunability factors ($\varepsilon(0)/\varepsilon(E)$ and $\mu(0)/\mu(E)$) for dielectric and magnetic permeability of BFO-BST are in the range of 1.22-1.27 and 1.18-1.19 respectively at 60 KV/cm biasing field.
- The change of dielectric constant and tangens losses is a result of oxygen vacancy formation during irradiation.

Thank You